Research Article

Synovial fluid proteomics and serum metabolomics reveal molecular and metabolic changes in osteoarthritis

Vishal Chandra[1]; Tashfeen Ashraf[2]; Pramod Yadav[1,3]*; Vikas Raghuvanshi[1,4]

[1]School of Life Sciences and Biotechnology, Chatrapati Shahu Ji Maharaj University Kanpur, Uttar Pradesh, India.

[2]School of Biotechnology, Gautam Buddha University, Greater Noida, India.

[3]Amity Institute of Neuropsychology and Neurosciences, Amity University Uttar Pradesh, India.

[4]Madurai Kamaraj University, Tamil Nadu, India.

*Corresponding Author: Pramod Yadav

Amity Institute of Neuropsychology and Neurosciences,

Amity University Uttar Pradesh, India.

Email: pramodyadavk3@gmail.com

Abbreviations: OA: Osteoarthritis; MS: Mass Spectrometry; 2DE: Two-Dimensional Gel Electrophoresis; SDS–PAGE: Sodium Dodecyl Sulfate–Polyacrylamide Gel Electrophoresis; NMR: Nuclear Magnetic Resonance; PCA: Principal Component Analysis; PLS-DA: Partial Least Squares-Discriminant Analysis; WHO: World Health Organization; K-L: Kellgren and Lawrence; WOMAC: Western Ontario and McMaster Universities Arthritis Index; VAS: Visual Analog Scale; ACR: American College of Rheumatology; DEAE: Diethylaminomethyl; SM: Synovial Membrane; MRI: Magnetic Resonance Imaging; RA: Rheumatoid Arthritis; VIP: Variable Importance in Projection; AUC: Area Under Curve; FDR: False Discovery Rate; HDL: High-Density Lipoproteins; LDL: Low-Density Lipoproteins; PUFA: Polyunsaturated Fatty Acids; ORA: Over-Representation Analysis; DAMPs: Damage-Associated Molecular Patterns; TLR-4: Toll-like Receptor 4.

Abstract

Background: Osteoarthritis (OA) is a common joint disorder with a complex and multifactorial pathogenesis. Proteomics analysis using two-dimensional gel electrophoresis (2DE) and mass spectrometry (MS) enables high-throughput identification of differentially expressed proteins related to OA. However, the etiology, pathophysiology, and early diagnostic markers of OA are still poorly understood.

Methods: Synovial fluid protein biomarkers were compared between OA patients and healthy controls. It was fractionated using DEAE cellulose and Sephadex G-200 columns, followed by SDS–PAGE and 2D-PAGE for visualization and identification. Mass spectrometry and Mascot were used for protein analysis, and serum metabolite profiles were also investigated using 1D 1H CPMG NMR spectra. Multivariate data analysis, including PCA and PLS-DA, was performed to detect metabolic differences between groups.

Results: Proteomics analysis revealed differential expression of synovial fluid proteins, such as serine protease inhibitors, complement components, and apolipoproteins, which may be involved in inflammation and cartilage breakdown. Additionally, serum metabolite profiles differed significantly between OA patients and controls, involving amino acid, lipid, glucose, and energy metabolism. The pathway analysis indicated disruption of the metabolic pathways associated with these metabolites.

Conclusions: This study provides insights into the molecular and metabolic changes in OA. Protein biomarkers and serum metabolite alterations enhance the understanding of OA pathogenesis and offer potential opportunities for early diagnosis and disease management. Further validation and translation of these findings into clinical applications are needed for improved OA detection and intervention strategies.

Introduction

Osteoarthritis (OA) is a degenerative joint disease that affects the articular cartilage, and its characteristics are increased friction, wear between bones, pain, swelling, stiffness and reduced mobility [1]. Among these, pain is a common symptom of OA, but its origin is unclear since cartilage lacks nociceptors. Morning stiffness is another symptom, but it lasts less than 30 minutes, and patients may also experience joint instability or locking [2,3]. According to the WHO, OA is expected to be the fourth leading cause of knee disability by 2024 [4]. Globally, more than 100 million people suffer from OA, and it has a higher prevalence in women than men [5]. The prevalence of knee OA increases with age and varies across regions, ranging from 7.5% in China [6] to 25% in northern Pakistan [7]. In India, OA is the second most prevalent rheumatologic problem, with a prevalence of 22% to 39%, and affects 60.6% of the urban population and 5.78% of the rural population [8]. Among people aged 65 years and above, OA accounts for 50% of all disability diseases [9]. The pathogenesis of OA is complex and multifactorial, involving the interaction of cartilage, subchondral bone, periosteum, joint capsule, and synovial fluid [10]. Physical examination is essential for diagnosis, and plain radiography can confirm OA in some cases, but advanced imaging techniques such as magnetic resonance imaging (MRI) are required for accurate diagnosis, especially if meniscal injury is suspected. However, these techniques are not affordable for many patients, resulting in underdiagnosis of OA. Despite considerable progress in OA research, its pathogenesis, etiology and progression remain poorly understood. Studies have reported abnormalities in the immune response and immune cells of OA patients, such as altered T-cell subsets. These abnormalities may play a role in the pathogenesis of OA and modulate the inflammatory response in the synovial membrane (SM), leading to cartilage degradation [11]. Despite extensive research with multiple approaches, our understanding of OA etiology and pathophysiology and our ability to diagnose it at an early stage are limited [12]. The present study was undertaken to investigate the comparative analysis of protein biomarkers occurring in the synovial fluid of patients and healthy controls.

Methodology

Inclusion and exclusion criteria of control and subject

We selected control subjects free of any clinical or radiological signs of joint disease, comorbidities, obesity, hypersensitivity, or cardiovascular disease. We used the Kellgren and Lawrence (K-L) score, the WOMAC score, the VAS score, and the American College of Rheumatology (ACR) classification to screen and evaluate OA patients. Only patients who met six or more criteria were included. Patients had knee pain (*asymmetrical*) lasting more than six months, stiffness (*less than 30 minutes*), swelling, cripitus, tenderness on the medical side of the joint, X-ray (*Grade II-78 and Grade III-22*), normal ligament stability, decreased motion, duration of symptoms (*3.3±1.49 years*), range of movements (*0-140/42±20.2*), VAS pain on movement (*4.7±1.4 cm*) and WOMAC score of patients (*difficulty 31.0±8.1; pain 9.2±2.2; stiffness 4.2±1.3 and total 44.2±9.8*). We excluded patients with infectious diseases such as diabetes mellitus, hypertension, thyroid dysfunction, neurological disorders, cancer, or other forms of arthritis. We also excluded patients with early OA (*<2 years from symptom onset*). The current study was approved by the Institutional Ethical Committee (*CSJMU/BSBT/BT/EC-20*), and all participants provided written informed consent.

Synovial fluid protein analysis

Synovial fluid was obtained from patients and healthy controls by an orthopedic doctor and diluted with 50 mM Tris-HCl buffer (pH 8). The diluted samples were stored at 4°C and applied to a DEAE cellulose column with a linear gradient of 0-500 mM NaCl (250 ml) at a flow rate of 84 ml/h. The fractions were collected and reapplied to a Sephadex G-200 column equilibrated with Tris-Cl buffer (50 mM and pH 7.4) and NaCl (100 mM) at a 45 ml/h flow rate. The eluted proteins were precipitated with ammonium sulfate, dissolved in a buffer with protease inhibitors, and used for SDS–PAGE and 2D-PAGE [13-16]. For the first dimension in 2D-PAGE, the protein concentration was determined by the Bradford method. Then, 200 μg of protein was mixed with 5 μl of 10% SDS and 5.3 μl of 1 M DTT, boiled at 100°C for 5 minutes, and placed on ice. Then, 100-120 μl of rehydration buffer (with 0.5 g of total protein extraction buffer, 0.5 ml of total protein extraction diluent, 50 μl of DTT, 100 μl of protease inhibitors, and 0.2% ampholytes) was added and loaded onto an IPG strip for active rehydration overnight. After 11-16 hours of active rehydration, the strip was removed, wiped off with tissue paper, and placed on the power pack with the correct orientation of electrodes (+/-). The strips were transferred to the top of 12% acrylamide denaturing gels for the second dimension. For silver staining, the gels were washed in water overnight, dehydrated with 50% ethanol three times, sensitized for 1 minute in sodium thiosulfate (0.02%), washed two times in water, impregnated in silver nitrate (0.2%) for 20 minutes, washed with distilled water for one minute, developed with 6% sodium carbonate under light with constant stirring and formaldehyde until the desired color intensity was achieved, washed with distilled water, terminated by adding 5% methanol and 7% acetic acid, and stored in 50% ethanol. For Coomassie blue staining, the gels were stained overnight with a solution containing 0.125% Coomassie blue R250, 50% methanol and 10% acetic acid, destained with the same solution without Coomassie blue R250, and stored in a solution containing 7% methanol and 10% acetic acid.

MS/MS and data analysis

Protein bands were in-gel digested with trypsin (modified sequencing grade; Promega, USA) according to the reported protocol [17]. The peptides were extracted, dried, desalted using ZipTip (Millipore, USA), and identified by nano-MS/MS. The peptides were reconstituted in 0.1% formic acid and subjected to LC–MS (Nano Advance, Bruker, Germany) and captive spray-Maxis-HD qTOF (Bruker, Germany) with high sensitivity and mass accuracy. The peptides were enriched in a nanotrap column (Bruker Magic C18AQ, particle size-5 μm, pore size-200 Å), separated on an analytical column (Bruker Magic C18AQ, 0.1 x 150 mm, 3 μm particle size and 200 Å pore size) at a flow rate of 800 nl/min and eluted using a linear gradient of 5-45% acetonitrile over 135 min [18]. The MS scan was performed in the 400-1400 m/z range, followed by an MS/MS scan of the six most intense precursor ions from the survey scan. Peak graphs were obtained by qTOF control (version 24.8) with the help of the Hystar postprocessing program and submitted to Protein

Scape software (Bruker, Germany), which uses Mascot (2.4.1 Matrix Science, UK). Mascot MS/MS ion search criteria were as follows: taxonomy Homo sapiens, trypsin digestion, allowing up to one missed cleavage, variable modification oxidation of methionine, fixed modification-cysteine as carboxyamidomethylation or propionamide, peptide tolerance of 50 ppm, and MS/MS tolerance of 0.05 Da. The "ion score cut-off" was set at 15 manually to eliminate the matches of lowest quality. To ensure the validity of the results, both protein and peptide identifications were subjected to a 1% FDR threshold [16].

Serum metabolite analysis

Serum samples were prepared by centrifuging clotted blood at 1200 rpm for 20 min at -4°C, aliquoting the supernatant, and storing it at -20°C. Prior to NMR analysis, serum samples were thawed, centrifuged at 10,000 rpm for 5 min to eliminate precipitates, and mixed with an equal volume of 0.9% saline sodium phosphate buffer (20 mM, pH 7.4) prepared in D_2O [19]. A coaxial insert containing 0.1% TSP (Sigma–Aldrich, Rhode Island, USA) in D_2O was used as an external standard reference for metabolite quantification. NMR spectra were acquired at 298 K on a Bruker Biospin Avance-III 800 MHz NMR spectrometer. Transverse relaxation edited CPMG spectra ID 1H NMR spectra [20] were recorded using the standard Bruker's pulse program library sequence (cpmgpr ID) with water peak presaturation during the RD of 5 s. Each spectrum had 128 scans and a total spin–spin relaxation time of 60 ms. FIDs were zero filled, Fourier transformed to 64 K data points, and manually phase and baseline corrected using Topspin-2.1. FIDs were processed with a 0.3 Hz line broadening and a sine-bell anodization prior to FT. The methyl peak of L-lactate (δ=1.33 ppm) served as the internal reference for chemical shifts. Spectra were visually examined and analysed multivariate to detect the changes in metabolic profiles. Chemical shifts were assigned by comparing them with the shifts available from MetaboMiner25 [21] and Chenomx (NMR suite, v8.1, Chenomx Inc., Edmonton, Canada). The assigned resonances were validated using *(a)* assigned resonances in 2D spectra for unambiguous assignment and *(b)* previously reported NMR assignments of metabolites, data obtained from the BMRB database and HMDB [22-24]. 2D 1H-1H TOCSY and 1H-13C HSQC NMR spectra were also acquired for some of the serum samples using the parameters described previously [25].

Results

Protein expression analysis by 2D-PAGE and MS/MS

The protein spots from the OA profile digested with trypsin were expunged from the 2D gel and analysed by MALDI-MS/MS. Many peptides and proteins were identified by searching the MascotTM database (Figure 1), and proteins were further classified according to the pathways in which they have major roles (Annexure 2). Annex 1 shows 29 differentially expressed proteins with a score of more than 15. No disease duration-dependent difference in the expression profile was observed. Mass spectrometric analysis indicated changes in the abundance of complement components C3 and C4b and the immunoglobulin constant region. These proteins may play a role in OA pathogenesis; however, no direct disease-specific proteins were detected in this study.

Serum metabolite expression analysis by 1D 1H CPMG NMR
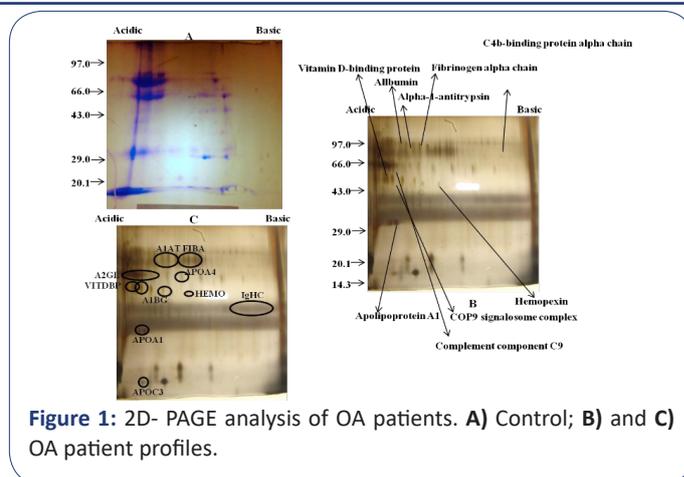

Figure 1: 2D- PAGE analysis of OA patients. **A)** Control; **B)** and **C)** OA patient profiles.

The spectra (Figure 3) displayed 1H NMR signals mainly from small metabolites with intense signals from lipoproteins, phospholipids, unsaturated lipids, choline metabolites, N-acetyl glycoproteins, glucose, lactate and amino acids. No major differences between the OA and control groups were observed by visual comparison. Hence, multivariate data analysis was performed on the NMR spectra to reveal the serum metabolic alterations caused by OA. The serum metabolic patterns of 10 grade II-III OA patients and sex-matched normal controls were analysed. The study subjects were selected to reduce the confounding variables (see Annexure 3). Figure 3 shows that the OA group was clearly discriminated from the control group along the PC1 direction, indicating distinct characteristics of OA serum. This method also detected outliers outside the 95% confidence region of the PCA model. We then applied the supervised clustering method PLS-DA to examine the subtle metabolic variations among the groups. The quality of each model was assessed by the parameters R2 and Q2, which are shown in the respective score plots in Figure 3(B). The model quality parameters R2 and Q2 were significantly high (R2, Q2>0.7), indicating satisfactory fit and good predictive power of the PLS-DA models (constructed from CPMG spectra). The PLS-DA score plots also showed that the OA and control groups were well clustered and separated, reflecting significant differences in the biochemical composition profiles of serum metabolites in OA patients and normal controls. The metabolites responsible for the discrimination were identified using the VIP and p<0.05 criteria. We identified 16 metabolites that were significantly perturbed in OA serum (VIP score ≥1) (see Figure 3 or Annexure 3).
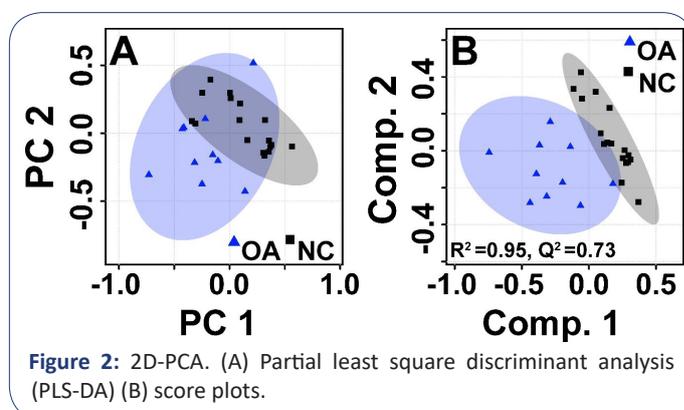

Figure 2: 2D-PCA. (A) Partial least square discriminant analysis (PLS-DA) (B) score plots.

CPMG spectra showing clear statistical separation between OA (represented by blue triangles) and normal control (NC) samples (represented by black squares). Each circle and triangle represent one subject. The validation parameters (R2 and Q2) corresponding to the PLS-DA model are also displayed in their score plots.
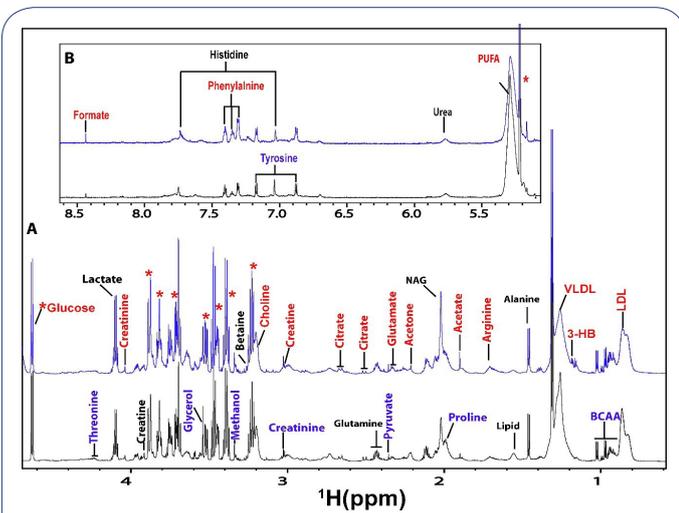
Figure 3: Stack plot of cumulative 1D 1H CPMG NMR spectra (A) from δ4.6–δ0.7 and (B) δ8.5–δ5.1 ppm) obtained for sera of OA patients (red) and normal controls (blue).
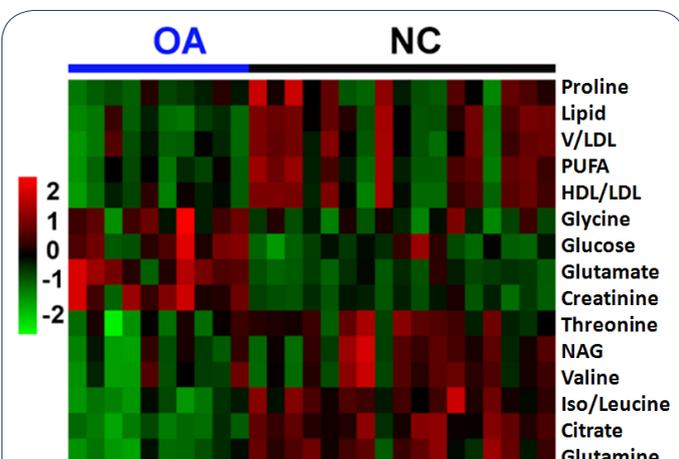

Figure 4: Heatmaps depicting z scores of 16 metabolites of OA patients and normal controls.

Heatmaps

Figure 4 shows the heatmaps for different metabolites that distinguish the OA group from the control group (upregulated and downregulated metabolites are shown in red and cyan, respectively). Consistent with our serological data, we found high serum creatinine and a low HDL/LDL ratio in OA by NMR analysis. OA is typically associated with dyslipidemia and has high serum creatinine and low uric acid, as identified by serological analysis. Using a nonparametric Mann–Whitney test, we quantified the differential abundance of metabolites and found that most of them were statistically significant ($p < 0.05$). The discriminating metabolic features were predominantly associated with lipid, amino acid, glucose and energy metabolism.

ROC curves

The area under the ROC curve reflects the discriminatory ability (0.5 indicates no discrimination; 1 indicates perfect discrimination). The AUC values ranged from 0.95 to 0.55 (Figure 5), indicating that these metabolites could be potential biomarkers for the clinical evaluation and surveillance of such patients. Figure 5 depicts representative ROC curves for some of the serum metabolites that exhibited significant changes in OA patients and their corresponding box plots (from the univariate analysis).
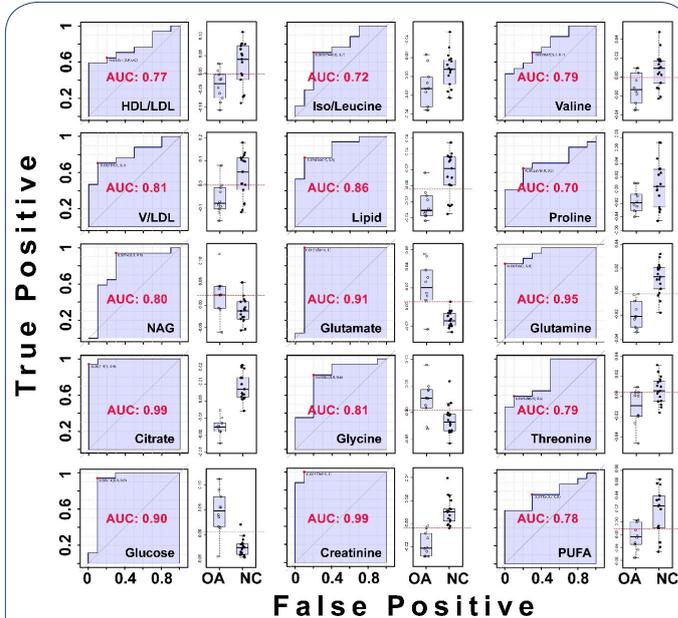

Figure 5: ROC curves along with their respective box plots.

Respective box plots of the significant metabolites that decreased or increased in the OA patients compared to the control group derived from the CPMG 1H NMR spectra. Boxes denote interquartile ranges, lines denote medians, and whiskers denote 10th and 90th percentiles.

Metabolic pathway by ORA

Figure 6 summarizes the pathway analysis and MSEA in MetaboAnalyst results. Five important metabolic pathways (protein biosynthesis, amino acid metabolism, glucose-energy metabolism) were found to be disturbed. The metabolic pathways associated with the identified combinations of metabolites are biased due to limited metabolites detected by NMR in the serum.
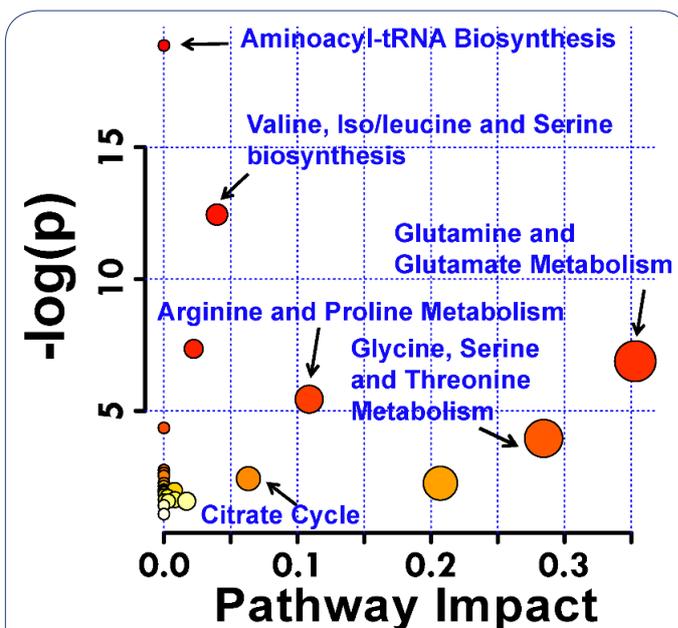

Figure 6: A diagram of a pathway impact by ORA.

The analysis was performed by using a pathway library restricted to Homo sapiens, and p values for ORA represent hypergeometric tests. Test p value (vertical axis, colour intensity) and impact factor (horizontal axis, circle size).

Discussion

Proteomics profile analysis by mass spectrometry

This study proposed that some proteins were overexpressed in OA patients, but none of these proteins were directly implicated in the pathophysiology of the disease (see Annexure 3). We identified several proteins, such as serine protease inhibitors, high levels of ATIII, and proteins related to lipid transport or protein binding, such as apolipoproteins, immunoglobulins, transmembrane proteins and transcriptional proteins. These proteins are involved in cartilage degradation or protein synthesis. Olsen et al. reported that the levels of APO-A1 in the synovial fluid of OA patients are higher due to diffusion and production by chondrocytes and FLSs [26]. Our results confirmed the role of APO-A1 in inflammation with increased expression of fibrinogen protein in OA and confirmed that these proteins can trigger TLR-4-dependent macrophage production of inflammatory cytokines and growth factors. This study reports high expression and activation of complement in OA joints. It also identified the proinflammatory complement components C3, C4b, and C9. C9 components from MAC were aberrantly expressed in OA, and C3 and C4b were higher in the early stage of OA. Hemopexin (HPX) is an acute phase protein that suppresses the adhesion of leukocytes and the release of cytokines from macrophages. Its high level suggests its role in OA. We also identified proteins involved in extracellular matrix, cartilage, and bone metabolism. Rab5 GDP/GTP exchange factor expression supports the role of the Ras superfamily in OA progression.

Metabolite analysis by NMR

The results of this study indicate that early metabolic changes in OA can be detected in serum by NMR. According to a study, degenerative joint disease can affect the synovium, as it becomes hypoxic [27]. This is also observed due to increased lactate concentration. This study found an increased creatinine concentration that indicates altered metabolism in early OA. Similar results have been reported for the serum metabolite profile in a sheep model of OA [28]. We observed increased glutamine and glutamate concentrations in the serum of OA patients. Glutamine confers chondrocyte resistance to heat stress and NO-mediated apoptosis [29]. Hence, glutamine elevation may reflect chondrocyte adaptation to various stressors during disease progression. Choline augmentation might indicate lipid catabolism from articular cartilage and leakage of its products into the bloodstream due to synovial membrane permeability enhancement. Alternatively, increased choline could result from the breakdown of Hoffa's pad or phospholipids in the joint [30]. We also found reduced leucine and histidine in the serum of OA patients. Comparison of spectral profiles of controls and patients reveals that cartilage breakdown continues with increased glycerol and hydroxybutyrate. Glycerol synthesis indicates triglyceride degradation in various tissues. Moreover, the decreased HDL/LDL ratio and PUFAs reflect the impact of free radical generation through lipid peroxidation, leading to high oxidative stress and inflammation [31].

Conclusion

Proteomics analysis using 2D-PAGE coupled with mass spectrometry revealed differentially expressed proteins involved in inflammation, oxidative stress, and the immune response, suggesting a complex interplay of factors in OA pathogenesis. NMR-based metabolomics analysis identified altered metabolic patterns in the serum of OA patients, indicating hypoxia, inflammation, and lipid metabolism disruption. Increased lactate and creatinine levels suggest tissue hypoxia and muscle breakdown near the affected joint. Alterations in amino acids, lipoproteins, and glucose-energy metabolism indicate disrupted metabolic pathways in OA patients. The integration of proteomics and metabolomics data provided a comprehensive view of the disease, highlighting potential targets for further investigation. The identified proteins and metabolites could serve as candidates for future diagnostic or prognostic biomarkers for OA. Further studies are needed to validate these findings and improve our understanding of OA pathophysiology and early detection.

References

1. Hunter DJ, Bierma-Zeinstra S. Osteoarthritis. The Lancet. 2019; 393: 1745-59. https://doi.org/10.1016/S0140-6736(19)30417-9.

2. Sibbritt D, Sundberg T, Ward L, Broom A, Frawley J, Bayes J, et al. What is the healthcare utilisation and out-of-pocket expenditure associated with osteoarthritis? A cross-sectional study. BMJ Open. 2022; 12. https://doi.org/10.1136/BMJOPEN-2021-055468.

3. Altman R, Asch E, Bloch D, Bole G, Borenstein D, Brandt K, et al. Development of criteria for the classification and reporting of osteoarthritis. Classification of osteoarthritis of the knee. Diagnostic and Therapeutic Criteria Committee of the American Rheumatism Association. Arthritis Rheum. 1986; 29: 1039-49. https://doi.org/10.1002/ART.1780290816.

4. WHO reveals leading causes of death and disability worldwide: 2000-2019 n.d. https://www.who.int/news/item/09-12-2020-who-reveals-leading-causes-of-death-and-disability-world-wide-2000-2019 (accessed July 24, 2023).

5. Thati S. Gender Differences in Osteoarthritis of Knee: An Indian Perspective. J Midlife Health. 2021; 12: 16. https://doi.org/10.4103/JMH.JMH_35_21.

6. Xiang YJ, Dai SM. Prevalence of rheumatic diseases and disability in China. Rheumatol Int. 2009; 29: 481-90. https://doi.org/10.1007/s00296-008-0809-z.

7. Farooqi A, Gibson T. Prevalence of the major rheumatic disorders in the adult population of north Pakistan. Br J Rheumatol. 1998; 37: 491-5. https://doi.org/10.1093/RHEUMATOLOGY/37.5.491.

8. Joshi VL, Chopra A. Is there an urban-rural divide? Population surveys of rheumatic musculoskeletal disorders in the Pune Region of India using the COPCORD Bhigwan model. Journal of Rheumatology. 2009; 36: 614-22. https://doi.org/10.3899/jrheum.080675.

9. Biehl M, Damm P, Trepczynski A, Preiss S, Salzmann GM. Towards planning of osteotomy around the knee with quantitative inclusion of the adduction moment: a biomechanical approach. J Exp Orthop. 2021; 8: 39. https://doi.org/10.1186/s40634-021-00324-3.

10. Chandnani VP, Ho C, Chu P, Trudell D, Resnick D. Knee hyaline cartilage evaluated with MR imaging: a cadaveric study involving multiple imaging sequences and intraarticular injection of gadolinium and saline solution. Radiology. 1991; 178: 557-61. https://doi.org/10.1148/RADIOLOGY.178.2.1987624.

11. Qiu G, Zhong S, Xie J, Feng H, Sun S, Gao C, et al. Expanded CD1c+CD163+ DC3 Population in Synovial Tissues Is Associated with Disease Progression of Osteoarthritis. J Immunol Res. 2022; 2022. https://doi.org/10.1155/2022/9634073.

12. Bhattacharjee M, Balakrishnan L, Renuse S, Advani J, Goel R, Sathe G, et al. Synovial fluid proteome in rheumatoid arthritis. Clin Proteomics. 2016; 13. https://doi.org/10.1186/S12014-016-9113-1.

13. Chandra DrV, Ashraf Dr (Mohd.) T, Yadav P, Raghuvanshi MrV. Gene Expression Profiles of Knee Osteoarthritis Patients and Healthy Controls: A Microarray Analysis Study. Preprint -SSRN. 2023. https://doi.org/10.2139/SSRN.4489650.

14. Yadav P. Challenges & Solutions for Recent Advancements in Multi-Drugs Resistance Tuberculosis: A Review. Microbiol Insights. 2023; 16: 1-9. https://doi.org/10.1177/11786361231152438.

15. Raghuvanshi V, Yadav P, Ali S. Interferon production by Viral, Bacterial & Yeast system: A comparative overview in 2023. Int Immunopharmacol. 2023; 120. https://doi.org/10.1016/j.intimp.2023.110340.

16. Rawat P, Bathla S, Baithalu R, Yadav ML, Kumar S, Ali SA, et al. Identification of potential protein biomarkers for early detection of pregnancy in cow urine using 2D DIGE and label free quantitation. Clin Proteomics. 2016; 13. https://doi.org/10.1186/S12014-016-9116-Y.

17. Habdous M, Vincent-Viry M, Visvikis S, Siest G. Rapid spectrophotometric method for serum glutathione S-transferases activity. Clinica Chimica Acta. 2002; 326: 131-42. https://doi.org/10.1016/S0009-8981(02)00329-7.

18. Bathla S, Rawat P, Baithalu R, Yadav ML, Naru J, Tiwari A, et al. Profiling of urinary proteins in Karan Fries cows reveals more than 1550 proteins. J Proteomics. 2015; 127:1 93-201. https://doi.org/10.1016/J.JPROT.2015.05.026.

19. Dona AC, Jiménez B, Schafer H, Humpfer E, Spraul M, Lewis MR, et al. Precision high-throughput proton NMR spectroscopy of human urine, serum, and plasma for large-scale metabolic phenotyping. Anal Chem. 2014; 86: 9887-94. https://doi.org/10.1021/AC5025039.

20. Tang H, Wang Y, Nicholson JK, Lindon JC. Use of relaxation-edited one-dimensional and two dimensional nuclear magnetic resonance spectroscopy to improve detection of small metabolites in blood plasma. Anal Biochem. 2004; 325: 260-72. https://doi.org/10.1016/j.ab.2003.10.033.

21. Xia J, Bjorndahl TC, Tang P, Wishart DS. MetaboMiner--semi-automated identification of metabolites from 2D NMR spectra of complex biofluids. BMC Bioinformatics. 2008; 9. https://doi.org/10.1186/1471-2105-9-507.

22. Nicholson JK, Foxall PJD, Spraul M, Farrant RD, Lindon JC. 750 MHz 1H and 1H-13C NMR Spectroscopy of Human Blood Plasma. Anal Chem. 1995; 67: 793-811. https://doi.org/10.1021/AC00101A004/ASSET/AC00101A004.FP.PNG_V03.

23. Guleria A, Bajpai NK, Rawat A, Khetrapal CL, Prasad N, Kumar D. Metabolite characterisation in peritoneal dialysis effluent using high-resolution (1) H and (1) H-(13) C NMR spectroscopy. Magn Reson Chem. 2014; 52: 475-9. https://doi.org/10.1002/MRC.4094.

24. Wishart DS, Jewison T, Guo AC, Wilson M, Knox C, Liu Y, et al. HMDB 3.0--The Human Metabolome Database in 2013. Nucleic Acids Res. 2013; 41. https://doi.org/10.1093/NAR/GKS1065.

25. Guleria A, Misra DP, Rawat A, Dubey D, Khetrapal CL, Bacon P, et al. NMR-Based Serum Metabolomics Discriminates Takayasu Arteritis from Healthy Individuals: A Proof-of-Principle Study. J Proteome Res. 2015; 14: 3372-81. https://doi.org/10.1021/ACS.JPROTEOME.5B00422.

26. Olsen AK, Sondergaard BC, Byrjalsen I, Tanko LB, Christiansen C, Müller A, et al. Anabolic and catabolic function of chondrocyte ex vivo is reflected by the metabolic processing of type II collagen. Osteoarthritis Cartilage. 2007; 15: 335-42. https://doi.org/10.1016/J.JOCA.2006.08.015.

27. Rice D, McNair PJ, Dalbeth N. Effects of cryotherapy on arthrogenic muscle inhibition using an experimental model of knee swelling. Arthritis Care Res (Hoboken). 2009; 61: 78-83. https://doi.org/10.1002/art.24168.

28. Maher AD, Coles C, White J, Bateman JF, Fuller ES, Burkhardt D, et al. 1H NMR spectroscopy of serum reveals unique metabolic fingerprints associated with subtypes of surgically induced osteoarthritis in sheep. J Proteome Res. 2012; 11: 4261-8. https://doi.org/10.1021/PR300368H/SUPPL_FILE/PR300368H_SI_001.PDF.

29. Tonomura H, Takahashi KA, Mazda O, Arai Y, Inoue A, Terauchi R, et al. Glutamine protects articular chondrocytes from heat stress and NO-induced apoptosis with HSP70 expression. Osteoarthritis Cartilage. 2006; 14: 545-53. https://doi.org/10.1016/J.JOCA.2005.12.008.

30. Lacitignola L, Fanizzi FP, Francioso E, Crovace A. 1H NMR investigation of normal and osteo-arthritic synovial fluid in the horse. Vet Comp Orthop Traumatol. 2008; 21: 85-8. https://doi.org/10.3415/VCOT-06-12-0101.

31. Yoshihara Y, Nakamura H, Obata K, Yamada H, Hayakawa T, Fujikawa K, et al. Matrix metalloproteinases and tissue inhibitors of metalloproteinases in synovial fluids from patients with rheumatoid arthritis or osteoarthritis. Ann Rheum Dis. 2000; 59: 455-61. https://doi.org/10.1136/ARD.59.6.455.